

# Uncertainties in constraining low-energy constants from ${}^3\text{H}$ $\beta$ decay

P. Klos,<sup>1,2,\*</sup> A. Carbone,<sup>1,2,†</sup> K. Hebeler,<sup>1,2,‡</sup> J. Menéndez,<sup>3,§</sup> and A. Schwenk<sup>1,2,4,¶</sup>

<sup>1</sup>*Institut für Kernphysik, Technische Universität Darmstadt, 64289 Darmstadt, Germany*

<sup>2</sup>*ExtreMe Matter Institute EMMI, GSI Helmholtzzentrum für Schwerionenforschung GmbH, 64291 Darmstadt, Germany*

<sup>3</sup>*Department of Physics, University of Tokyo, Hongo, Tokyo 113-0033, Japan*

<sup>4</sup>*Max-Planck-Institut für Kernphysik, Saupfercheckweg 1, 69117 Heidelberg, Germany*

We discuss the uncertainties in constraining low-energy constants of chiral effective field theory from  ${}^3\text{H}$   $\beta$  decay. The half-life is very precisely known, so that the Gamow-Teller matrix element has been used to fit the coupling  $c_D$  of the axial-vector current to a short-range two-nucleon pair. Because the same coupling also describes the leading one-pion-exchange three-nucleon force, this in principle provides a very constraining fit, uncorrelated with the  ${}^3\text{H}$  binding energy fit used to constrain another low-energy coupling in three-nucleon forces. However, so far such  ${}^3\text{H}$  half-life fits have only been performed at a fixed cutoff value. We show that the cutoff dependence due to the regulators in the axial-vector two-body current can significantly affect the Gamow-Teller matrix elements and consequently also the extracted values for the  $c_D$  coupling constant. The degree of the cutoff dependence is correlated with the softness of the employed NN interaction. As a result, present three-nucleon forces based on a fit to  ${}^3\text{H}$   $\beta$  decay underestimate the uncertainty in  $c_D$ . We explore a range of  $c_D$  values that is compatible within cutoff variation with the experimental  ${}^3\text{H}$  half-life and estimate the resulting uncertainties for many-body systems by performing calculations of symmetric nuclear matter.

PACS numbers: 21.30.-x, 21.45.Ff, 23.40.-s, 27.10.+h

*Introduction.* The development of new and improved nuclear forces within chiral effective field theory (EFT) is currently a very active field of research [1–4]. In contrast to phenomenological approaches, chiral EFT provides a framework that allows to systematically derive improvable expansions for nucleon-nucleon (NN) and many-body forces as well as electroweak current operators at low energies [5–8]. Within Weinberg’s power counting scheme [9] the contributions to NN forces have been worked out up to fifth order in the chiral expansion [3, 10], whereas three-nucleon (3N) and four-nucleon forces have been developed up to fourth order [11–14]. Similarly nuclear currents have been derived up to fourth order for axial-vector [15, 16] and vector currents [17–21].

The contributions to nuclear forces and currents generally depend on low-energy couplings (LECs) that capture the short-distance physics that is not resolved explicitly within the EFT. Therefore, to determine the LECs, fits to data are needed. Up to second (next-to-leading) order there are no contributions from many-body interactions or currents, and the LECs in the NN forces are usually obtained by fits to pion-nucleon and nucleon-nucleon scattering data. At third (next-to-next-to leading) order,  $\text{N}^2\text{LO}$ , two additional LECs,  $c_D$  and  $c_E$ , enter in 3N forces and two-body (2b) currents. While  $c_D$  enters in both the NN-contact-one-pion exchange 3N force and the

coupling of a NN pair to an axial-vector probe,  $c_E$  only parameterizes the 3N short-range contact interaction.

Different strategies have been employed to determine the values of the 3N LECs up to  $\text{N}^2\text{LO}$ . If only the new couplings appearing at this order are to be fixed, two observables are needed. One popular choice, first introduced in Ref. [22], is to determine  $c_D$  and  $c_E$  by fits to the binding energy of  ${}^3\text{H}$  (triton) or  ${}^3\text{He}$ , and the  ${}^3\text{H}$   $\beta$ -decay half-life. This procedure, also used in other studies [23, 24], has recently been extended by including selected terms up to fifth order in the nuclear currents [25]. On the other hand, in Ref. [26]  $c_D$  and  $c_E$  were fixed by fits to the  ${}^3\text{H}$  binding energy and the  ${}^4\text{He}$  charge radius. Moreover, different pairs of data have been chosen to determine  $c_D$  and  $c_E$ , such as the  ${}^3\text{H}$  binding energy and the neutron-deuteron scattering length [27], or the  ${}^4\text{He}$  binding energy and the  $P$ -wave spin-orbit splitting in neutron- ${}^4\text{He}$  scattering [28]. An alternative strategy was employed in Ref. [4], following similar ideas as in Ref. [2]. Instead of fitting the NN and 3N interactions separately, all LECs up to a given order in the chiral expansion were fit simultaneously based on a  $\chi^2$  minimization in a large parameter space. The correlations between different LECs were also studied systematically.

Generally, reliable fits require observables that are not strongly correlated under variations of the LECs. In particular, for the  $c_D$  and  $c_E$  determination, Ref. [22] showed that this condition is fulfilled for fits to the  ${}^3\text{H}$  half-life and binding energy, as proposed earlier [29]. With the LECs fixed, heavier systems can be studied. The interactions based on Ref. [22] provide good nuclear structure properties, including binding energies, up to oxygen isotopes [30–32], but tend to overbind heavier nuclei [31, 33–35]. The significance of the overbinding is un-

\* E-mail: pklos@theorie.ikp.physik.tu-darmstadt.de

† E-mail: arianna@theorie.ikp.physik.tu-darmstadt.de

‡ E-mail: kai.hebeler@physik.tu-darmstadt.de

§ E-mail: menendez@nt.phys.s.u-tokyo.ac.jp

¶ E-mail: schwenk@physik.tu-darmstadt.de

clear, however, because the uncertainties associated to the interactions have not been systematically explored. Other interactions fitted to different data lead to promising results for heavier nuclei, neutron and nuclear matter [2, 26, 28, 31, 36–43].

In this work, we investigate the theoretical uncertainties of LEC determinations involving the  ${}^3\text{H}$  half-life and study to what extent the LECs can be constrained based on these fits. Presently, a major source of uncertainty that has not yet been properly taken into account is the regularization scheme and scale dependence for both nuclear interactions and currents. So far, two different regulators in momentum space have been used: first, local regulators that affect all matrix elements in the momentum transfer; and second, nonlocal regulators that act on the relative momenta in the initial and final states. The consistent and efficient choice of a regulator scheme is subject of an active ongoing debate as various different schemes and scales are currently used for nuclear interactions [1, 3, 4, 44, 45]. Given that nuclear structure observables are already sensitive to a specific choice (see, e.g., Refs. [46, 47]) the consistent treatment of regulators in interactions and currents represents an additional challenge. First studies concerned with the uncertainty due to the choice of regulators were performed only for a relatively small range of cutoff values [48, 49]. In this paper we show that the regulator choice can affect significantly the LEC values extracted from  ${}^3\text{H}$   $\beta$  decay. This finding raises the fundamental question regarding the consistency of the regularization scheme in nuclear interactions and currents.

*Triton  $\beta$  decay and nuclear currents.* Formally, the half-life  $t$  for the  $\beta$  decay of  ${}^3\text{H}$  can be expressed in the form [50, 51]

$$(1 + \delta_R)t = \frac{K/G_V^2}{f_V \langle F \rangle^2 + f_A g_A^2 \langle \text{GT} \rangle^2}, \quad (1)$$

where  $\delta_R$  includes radiative corrections that originate from virtual photon exchange between the charged particles,  $f_V$  and  $f_A$  are Fermi functions, which account for the deformation of the electron wave function due to electromagnetic interactions with the nucleus, and  $G_V = 1$  and  $g_A = 1.27$  denote the vector and axial-vector couplings. The kinematics of the process leads to an additional constant  $K = 2\pi^3 \ln 2/m_e^5$ , where  $m_e$  is the electron mass. The half-life depends on the nuclear matrix elements of the vector and axial-vector currents denoted as Fermi (F) and Gamow-Teller (GT) matrix elements, respectively. The Fermi reduced matrix element is given by  $\langle F \rangle = \langle {}^3\text{He} | \sum_{i=1}^3 \tau_i^+ | {}^3\text{H} \rangle$ , where  $\tau^+ = \frac{1}{2}(\tau^x + i\tau^y)$  is the isospin-raising operator. The Gamow-Teller reduced matrix element contains axial-vector one-body (1b) and 2b current contributions:

$$\langle \text{GT} \rangle = \frac{1}{g_A} \langle {}^3\text{He} | \sum_{i=1}^3 \mathbf{J}_{i,1b}^+ + \sum_{i<j} \mathbf{J}_{ij,2b}^+ | {}^3\text{H} \rangle. \quad (2)$$

The axial-vector current was derived in chiral EFT to third order [52–54], also denoted as  $Q^3$ , where  $Q \sim m_\pi$

is the typical momentum scale, of the order of the pion mass, and the expansion refers to powers in  $Q/\Lambda_b$ , with  $\Lambda_b \sim 500$  MeV the breakdown scale of the EFT. More recent derivations have been performed to order  $Q^4$  [15, 16]. Since the  $Q$ -value of the  ${}^3\text{H}$   $\beta$  decay is about 100 keV, to very good approximation we evaluate all currents at vanishing momentum transfer. Therefore to order  $Q^0$  and  $Q^2$ , only the momentum-independent 1b current contributes:

$$\mathbf{J}_{i,1b}^+ = g_A \tau_i^+ \boldsymbol{\sigma}_i. \quad (3)$$

At order  $Q^3$ , 2b currents enter. In the limit of vanishing momentum transfer, they are given by [52, 54]

$$\begin{aligned} \mathbf{J}_{12,2b}^+ = & -\frac{g_A}{2F_\pi^2} \frac{1}{\mathbf{k}^2 + m_\pi^2} \left[ 4c_3 \mathbf{k} \mathbf{k} \cdot (\tau_1^+ \boldsymbol{\sigma}_1 + \tau_2^+ \boldsymbol{\sigma}_2) \right. \\ & + \left( c_4 + \frac{1}{4m_N} \right) (\boldsymbol{\tau}_1 \times \boldsymbol{\tau}_2)^+ \mathbf{k} \times [(\boldsymbol{\sigma}_1 \times \boldsymbol{\sigma}_2) \times \mathbf{k}] \\ & - \frac{i}{8m_N} (\boldsymbol{\tau}_1 \times \boldsymbol{\tau}_2)^+ (\mathbf{p}_1 + \mathbf{p}'_1 - \mathbf{p}_2 - \mathbf{p}'_2) (\boldsymbol{\sigma}_1 - \boldsymbol{\sigma}_2) \cdot \mathbf{k} \left. \right] \\ & - 2id_1 (\tau_1^+ \boldsymbol{\sigma}_1 + \tau_2^+ \boldsymbol{\sigma}_2) - id_2 (\boldsymbol{\tau}_1 \times \boldsymbol{\tau}_2)^+ (\boldsymbol{\sigma}_1 \times \boldsymbol{\sigma}_2), \end{aligned} \quad (4)$$

where  $(\boldsymbol{\tau}_1 \times \boldsymbol{\tau}_2)^+ = (\tau_1 \times \tau_2)^x + i(\tau_1 \times \tau_2)^y$ ,  $\mathbf{k} = (\mathbf{k}_2 - \mathbf{k}_1)/2$ ,  $\mathbf{k}_i = \mathbf{p}'_i - \mathbf{p}_i$ , with initial and final nucleon momenta  $\mathbf{p}_i$  and  $\mathbf{p}'_i$ , and the pion decay constant  $F_\pi = 92.4$  MeV. We use  $m_\pi = 138$  MeV and for the nucleon mass  $m_N = 938.9$  MeV. The  $c_i$  are pion-nucleon LECs, which we take consistently with the corresponding nuclear interaction.

The relativistic corrections of the leading 2b currents are suppressed by a factor of  $1/m_N$ . In our counting this factor leads to an increase of the chiral order by two units since  $Q/m_N \sim (Q/\Lambda_b)^2$ . Therefore, relativistic corrections to 2b currents are of order  $Q^4$ . Nevertheless we include the  $1/(4m_N)$  correction term of  $c_4$  in Eq. (4) in order to be consistent with Ref. [22], but its effect is minor. Similarly, the contribution of the term proportional to  $i/(8m_N)$  is only about 0.001% of the total Gamow-Teller matrix element and can thus be neglected.

Antisymmetrization of the short-range part of the 2b currents allows to express  $d_1$  and  $d_2$  in terms of one linear combination  $c_D = \Lambda_\chi F_\pi^2 (d_1 + 2d_2)$  with  $\Lambda_\chi = 700$  MeV [52].\* The coupling  $c_D$  describes the strength of a pion or an axial-vector current interacting with a short-range NN pair. This relation is a generalization of the Goldberger-Treiman relation to the 2b level [29]. The total strength  $d_R$  of the short-range part includes contributions from  $c_3$ ,  $c_4$  and the minor relativistic correction:

$$d_R = \frac{1}{\Lambda_\chi g_A} c_D + \frac{1}{3} (c_3 + 2c_4) + \frac{1}{6m_N}. \quad (5)$$

*Nuclear states and regulators.* We evaluate the Fermi and Gamow-Teller matrix elements in a momentum-space partial-wave representation. For this we calculate

\* Note that this is no longer strictly the case for local regulators.

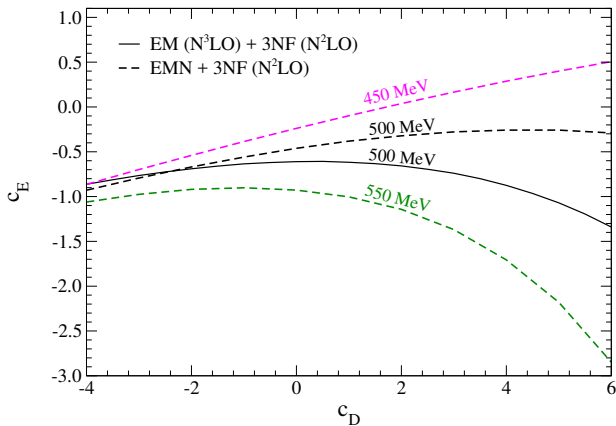


FIG. 1. Values for the low-energy couplings  $c_D$  and  $c_E$  that reproduce the  ${}^3\text{H}$  binding energy using the EM 500 MeV  $\text{N}^3\text{LO}$  potential of Ref. [44] plus 3N interactions at order  $\text{N}^2\text{LO}$  (solid), and using the EMN potentials of Ref. [55] plus consistent 3N interactions at order  $\text{N}^2\text{LO}$  (dashed) for different cutoff values.

${}^3\text{H}$  and  ${}^3\text{He}$  by solving the Faddeev equations in a partial-wave momentum basis using different chiral NN interactions at both  $\text{N}^2\text{LO}$  and  $\text{N}^3\text{LO}$  plus 3N interactions at  $\text{N}^2\text{LO}$ . Specifically, we use a  $Jj$ -coupled three-body basis of the form

$$|pq\alpha\rangle = |pq; [(LS)J(ls)j] \mathcal{J} \mathcal{J}_z (Tt) \mathcal{T} \mathcal{T}_z\rangle, \quad (6)$$

where  $L$ ,  $S$ ,  $J$  and  $T$  denote the relative orbital angular momentum, spin, total angular momentum and isospin of particles 1 and 2 with relative momentum  $p$ . The single-particle quantum numbers  $l$ ,  $s = 1/2$ ,  $j$  and  $t = 1/2$  label the orbital angular momentum, spin, total angular momentum and isospin of particle 3 with momentum  $q$  relative to the center-of-mass of particles 1 and 2. In this paper all calculations for  ${}^3\text{H}$  and  ${}^3\text{He}$  are performed using the averaged neutron-proton mass  $m = 1/2(m_n + m_p)$  for all three particles. This approximation is known to provide binding energy results within 10 keV of the full results [56]. In this approximation the three-body total angular momentum and isospin of the ground states take the values  $\mathcal{J} = \mathcal{T} = 1/2$ , with magnetic projections  $\mathcal{J}_z$  and  $\mathcal{T}_z$ , and we include all partial waves up to two-body  $J_{\max} = 6$ .

For the calculation of the nuclear states we fix the value of  $c_E$  for a given value of  $c_D$  by fitting the binding energy of  ${}^3\text{H}$  to the experimental value  $E_{3\text{H}} = -8.482$  MeV. The resulting LEC values are shown in Fig. 1 for the calculation based on the NN interaction at  $\text{N}^3\text{LO}$  of Ref. [44] (EM 500 MeV) combined with 3N forces at  $\text{N}^2\text{LO}$  (solid line). Here we used a non-local three-body regulator of the form  $f_{3\text{N}}(p, q, n_{\text{exp}}) = \exp[-(p^2 + 3/4q^2)/\Lambda_{3\text{N}}^2]^{n_{\text{exp}}}$  with  $\Lambda_{3\text{N}} = 500$  MeV and  $n_{\text{exp}} = 3$ . Furthermore, we performed fits based on the potentials of Ref. [55] (EMN) at order  $\text{N}^2\text{LO}$  including the consistent 3N (with same  $c_i$ ) force contributions at this order for cutoff values of

450 MeV, 500 MeV, and 550 MeV (dashed lines) and  $n_{\text{exp}} = 4$ . Figure 1 shows that the  $c_E$  values are of natural size for the entire range of  $c_D$  values and all employed NN interactions.

The choice of regulator should be considered carefully when studying transition operators such as  $\beta$  decay. Generally, any nuclear interaction contains intrinsic resolution scales  $\Lambda$  that separate the low-energy degrees of freedom that are treated explicitly from the high-energy degrees of freedom that are contained implicitly in the coupling constants. As a result, the  ${}^3\text{H}$  and  ${}^3\text{He}$  wave functions contain these resolution scales and are hence suppressed at momenta that lie well beyond them. For the fit results shown in Fig. 1 the cutoff scales  $\Lambda_{3\text{N}}$  were chosen to be the same as in the corresponding NN interactions. When evaluating expectation values of operators with respect to these wave functions the fundamental question arises on how the high-momentum components of the operators need to be regularized. In Ref. [22] the 2b current operators were regularized by local regulators of the form

$$f_{\Lambda}^{\text{loc}}(\mathbf{p}, \mathbf{p}') = \exp[-(\mathbf{p} - \mathbf{p}')^4/\Lambda^4], \quad (7)$$

where  $\mathbf{p}$  and  $\mathbf{p}'$  denote the relative momenta in the initial and final state. In contrast the NN interactions derived in Refs. [44, 55, 57] have been regularized using a different, non-local regulator of the form

$$f_{\Lambda}^{\text{non-loc}}(p^2, p'^2) = \exp[-(p^{2n} + p'^{2n})/\Lambda^{2n}]. \quad (8)$$

*Results.* First we calculate the Fermi matrix element and obtain  $\langle F \rangle = 0.9998$  for all potentials from Ref. [44] independently of the LECs in the 3N force, in good agreement with isospin conservation and previous calculations [25, 50]. We then focus on the Gamow-Teller matrix element, which can be fitted to the  ${}^3\text{H}$  half-life using Eq. (1). We represent all terms of Eq. (4) in the partial-wave basis and evaluate the reduced matrix element in Eq. (2). Figure 2 shows results for the Gamow-Teller matrix elements as a function of the  $c_D$  values, evaluated for different cutoff values  $\Lambda$  in the 2b current regulators of Eqs. (7) and (8). We use no regulator for the 1b current, consistently with the calculation of  $\langle F \rangle$ . Our results are presented in terms of the ratio of the calculated and the experimental matrix element  $\langle \text{GT} \rangle_{\text{exp}} = \sqrt{3} \cdot 0.956$ , which reproduces the measured  ${}^3\text{H}$  half-life [22]. For each cutoff value, we show results based on calculations including 3N forces (solid lines) and without 3N forces (dashed lines) using for the 2b currents the local regulator of Eq. (7). In addition we show results using the non-local regulator of Eq. (8) in the 2b current. For comparison we also show results including only 1b currents [see Eq. (3)]. This approximation underpredicts the experimental value by about 2%, which demonstrates the need for a small 2b-current contribution. For comparison, Fig. 3 shows the corresponding Gamow-Teller matrix elements as a function of the  $c_D$  values for the different EMN potentials plus 3N interactions at  $\text{N}^2\text{LO}$ .

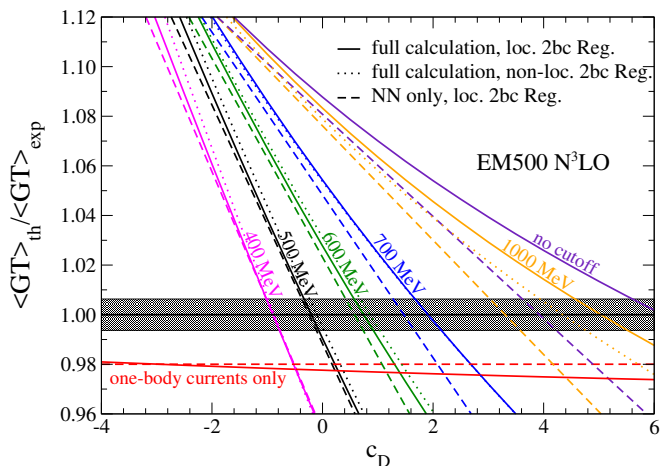


FIG. 2. (Color online) Ratio of calculated and experimental Gamow-Teller matrix elements as a function of  $c_D$  for different cutoff values and regulators in the two-body currents, based on the EM 500 MeV  $N^3$ LO potential of Ref. [44]. The solid (dotted) lines show results for nuclear states including 3N forces at  $N^2$ LO using the  ${}^3\text{H}$  binding energy constraint of Fig. 1 for a local [non-local with  $n = 2$ , see Eq.(8)] regulator in the two-body currents. For comparison, we also show results based on NN interactions only (dashed lines) and with 1b currents only. The width of the shaded band denotes the  $2\sigma$  experimental uncertainty.

Figures 2 and 3 show that for each cutoff value the Gamow-Teller matrix elements exhibit a strong  $c_D$  dependence, which indicates the small degree of correlation between the  ${}^3\text{H}$  binding energy and lifetime and in principle allows for a precise determination of  $c_D$  by fitting to the experimental  $\langle \text{GT} \rangle_{\text{exp}}$  value. However, the inferred  $c_D$  values also depend sensitively on the regulator applied to the current operator. While the cutoff  $\Lambda = 400$  MeV in Fig. 2 yields a value of  $c_D = -0.9$ , a maximal value of  $c_D = 6.0$  is found for unregularized current operators. In the latter case the contributions of the current operator are cut off at high momenta solely by the nuclear states. For  $\Lambda = 500$  MeV we reproduce the result of Ref. [22] of  $c_D = -0.24$  for a local regulator of the form Eq.(7). Note that for these calculations a non-local regulator was used for the NN interactions and a local regulator for the currents. Replacing the regulator in the 2b currents by a non-local one yields only slight changes in the curves and consequently very similar  $c_D$  values. In addition, Fig. 2 also shows that the sensitivity of the Gamow-Teller matrix elements on 3N forces depends significantly on the cutoff value. While for small cutoffs the fitted values for  $c_D$  are to very good approximation independent of 3N interactions (as argued in Ref. [22]), for  $\Lambda \gtrsim 600$  MeV the fits start to become sensitive to contributions from 3N forces.

Figure 3 shows the corresponding results for the  $c_D$  ranges based on the EMN NN interactions plus 3N interactions at  $N^2$ LO. The solid lines show the results using

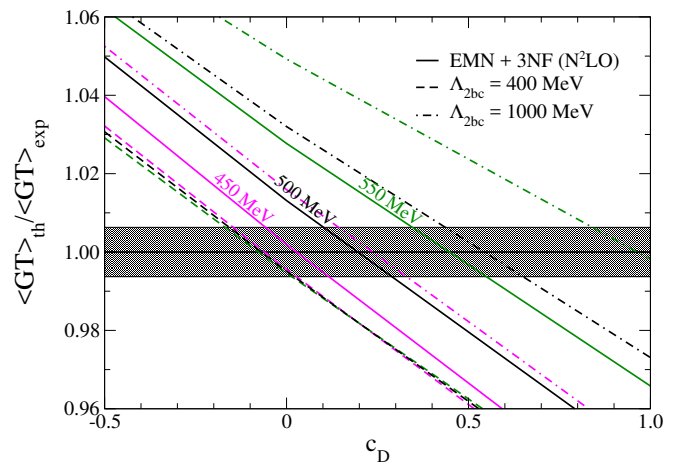


FIG. 3. (Color online) Ratio of calculated and experimental Gamow-Teller matrix elements as a function of  $c_D$  based on the EMN potentials at order  $N^2$ LO of Ref. [55]. We show results for the 2b current cutoff  $\Lambda_{2bc} = 400$  MeV (dashed lines) and  $\Lambda_{2bc} = 1000$  MeV (dash-dotted lines) using a non-local regulator [see Eq.(8)] with  $n = 2$ , whereas the solid lines show the cases when using the same cutoff values in the regulators for the interactions and currents. The width of the shaded band denotes the  $2\sigma$  experimental uncertainty.

the same cutoff values in the non-local regulators for the currents and the NN and 3N interactions. The dashed and dash-dotted lines are generated by changing the cutoff values for the currents to 400 MeV and 1000 MeV, respectively. The reduced sensitivity of the  $c_D$  values on the cutoff values compared to the results of Fig. 2 can be traced back to the enhanced perturbativeness of the EMN potentials compared to the previous EM 500 MeV potential [58]. In particular, we found that contributions in the three-body wave functions for the latter interaction extend to much higher momenta and consequently a regulator has a stronger impact on the results for small cutoff values.

These results highlight that the sensitivity of the Gamow-Teller matrix elements on the regulators used for both forces and current operators can lead to significant uncertainties for the extracted values of  $c_D$ . This sensitivity has also been studied in Refs. [23, 25, 48, 49]. Taking into account the different regularization schemes used in these works the obtained  $c_D$  variation is of similar size to the one we found for the EMN potentials shown in Fig. 3. Still, it is not obvious how a consistent choice of regulators can be precisely defined in this context, especially when the form of the employed regulator is different for forces and currents, as is the case for the results using the local regulator shown in Fig. 2. Until these consistency constraints are taken into account it is crucial to include the uncertainties due to the regulator dependence when fitting LECs to the  $\beta$  decay of  ${}^3\text{H}$ .

Given the different possible observables used to determine  $c_D$  and  $c_E$  the question arises to what extent these

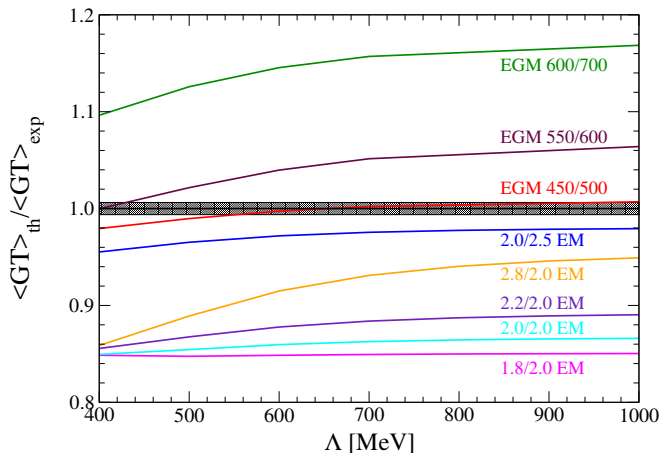


FIG. 4. (Color online) Ratio of calculated and experimental Gamow-Teller matrix elements as a function of the cutoff  $\Lambda$  in the non-local regulator [ $n = 2$ , see Eq. (8)] for a set of chiral interactions, using different fitting observables: the results labeled 'EM' are based on NN plus 3N interactions, for which the  $c_D$  and  $c_E$  values are fit to the binding energy of  ${}^3\text{H}$  and the charge radius of  ${}^4\text{He}$  (see Ref. [26] for details). The results labeled 'EGM' are based on NN plus 3N forces fitted to the binding energy of  ${}^3\text{H}$  and the neutron-deuteron scattering length [59]. The width of the shaded band denotes the  $2\sigma$  experimental uncertainty.

fits are compatible with extractions from the  ${}^3\text{H}$   $\beta$  decay. Figure 4 shows the results for the Gamow-Teller matrix elements as a function of the 2b current cutoff for interactions fitted to the binding energy of  ${}^3\text{H}$  and the charge radius of  ${}^4\text{He}$  [26] (denoted as EM), as well as interactions fitted to the binding energy of  ${}^3\text{H}$  and the neutron-deuteron scattering length [27] (EGM). The different EGM interactions are labeled by the value of the internal resolution scales in MeV (see Ref. [59] for details), whereas the EM interactions are labeled by the similarity-renormalization-group resolution scale in units of  $\text{fm}^{-1}$  (see Ref. [26] for details). Again, we find that the sensitivity of the results on the cutoff  $\Lambda$  tends to become stronger with increasing resolution scales and reduced perturbativeness. Second, in general it is not possible to reproduce the experimental value of the  ${}^3\text{H}$   $\beta$ -decay Gamow-Teller matrix element based on LECs extracted from fits to other observables, even when the cutoff dependence of the results is taken into account. This discrepancy might be caused by the application of chiral forces and currents at different chiral orders as suggested in Ref. [25] and also suggests that the uncertainty of the  ${}^3\text{H}$   $\beta$  decay half-life is larger than the effect from 2b currents, especially at  $\text{N}^2\text{LO}$ .

We also note that fitting the Gamow-Teller matrix element within experimental uncertainties neglects the fact that the calculations are constrained to a particular chiral order, which can be associated with an uncertainty due to the truncation in the chiral expansion (e.g., for recent work, see Refs. [62, 63]). This illustrates, in agreement

with the main result of this work, that previous works have underestimated the uncertainties when fitting LECs to the triton half-life. We leave such consistent order by order calculations to future work.

Based on the obtained uncertainty ranges for  $c_D$  and  $c_E$  we also explore the resulting uncertainties for many-body observables by calculating the energy per nucleon of symmetric nuclear matter within the self-consistent Green's function framework [60]. In this nonperturbative many-body approach 3N forces are included via a normal-ordering procedure with respect to the fully correlated reference state [60, 64]. Figures 5 and 6 show the energy per nucleon  $E/A$  of symmetric nuclear matter as a function of the density  $\rho$  using the NN and 3N interactions used in Figs. 2 and 3, respectively. For the EM 500 MeV potential we find a strong dependence on the  $c_D$  and  $c_E$  values corresponding to different cutoff values in the local regulator of the 2b currents. The saturation energy ranges from  $E/A \sim -11$  MeV, for smaller cutoffs, to  $E/A \sim -21$  MeV, for the LECs corresponding to the unregularized 2b current. For cutoffs in the range  $\Lambda = 400 - 700$  MeV, the saturation density takes the values  $\rho \sim 0.13 - 0.15 \text{ fm}^{-3}$ . Performing corresponding calculations using the EMN potentials we find a smaller dependence on the cutoff values. In Fig. 6 we show results for different values of  $c_D$  and  $c_E$  as obtained from the fit to the Gamow-Teller matrix element in Fig. 3. First, we notice that the variation with respect to change in the 2b current cutoff grows with increasing cutoff value of the interaction. This is related to the increasing range of  $c_D$  values obtained in Fig. 3. Furthermore, the variation due to the change of the 2b current cutoff of the 500 MeV EMN potential is much smaller than in Fig. 5 for the EM 500 MeV potential. As mentioned before this can be explained by the enhanced perturbativeness of the EMN potentials. However, as the potentials become less perturbative, which is the case for the  $\Lambda = 550$  MeV potential, the variation increases highlighting the relevance of the 2b current cutoff. Finally, we state that for all EMN potentials it is not possible to reproduce the saturation point based on the fits to the  ${}^3\text{H}$   $\beta$  decay.

These results indicate that the uncertainties of the LECs due to the regulator dependence of the nuclear forces and currents can lead to significant uncertainties for nuclear structure observables. The observed dependence may also be related to possible inconsistencies in the power counting in the currents due to the non-trivial enhancement of some contributions [65]. In order to systematically reduce these uncertainties more detailed studies are required to find a consistent way of regularizing nuclear interactions and currents ensuring also the continuity equation. In Ref. [15] it was shown that the currents and interactions indeed fulfill the continuity equation at the operator level, i.e., for infinite cutoffs. Generalizing this analysis to regularized matrix elements will provide additional nontrivial constraints for a consistent way of regularizing electroweak currents.

*Summary.* We have studied the uncertainties in con-

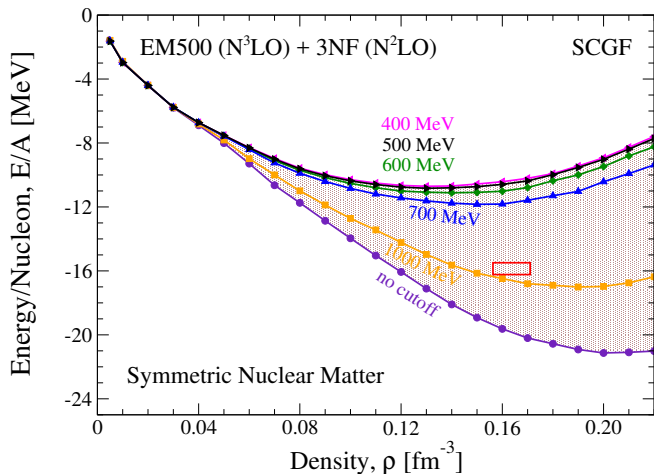


FIG. 5. (Color online) Energy per nucleon of symmetric nuclear matter as a function of nucleon density obtained within the self-consistent Green’s function approach [60]. Results are based on the NN EM 500 MeV at  $N^3\text{LO}$ , including normal-ordered 3N interaction contributions at  $N^2\text{LO}$ . The curves correspond to different  $c_D$  and  $c_E$  values obtained according to Figs. 1 and 2. The box describes the range for the empirical saturation point provided by mean-field calculations [61].

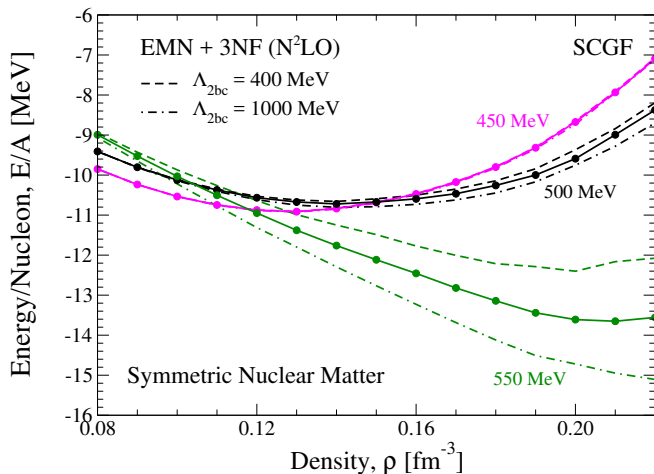


FIG. 6. (Color online) Same as Fig. 5 but showing results based on the EMN potentials at  $N^2\text{LO}$ . The curves correspond to different  $c_D$  and  $c_E$  values obtained according to Figs. 1 and 3. The different lines correspond to 2b currents cutoffs equivalent to the interaction (solid),  $\Lambda_{2bc} = 400$  MeV (dashed), and  $\Lambda_{2bc} = 1000$  MeV (dash-dotted) as shown in Fig. 3.

straining the LECs of the leading-order 3N interactions,  $c_D$  and  $c_E$ , via fits to  ${}^3\text{H}$   $\beta$  decay. We found that the extracted values of  $c_D$  generally exhibit a significant dependence on the cutoff scale used for the currents, whereas the degree of uncertainty is correlated to the perturbativeness of the employed nuclear interactions. These additional uncertainties need to be taken into account when including 3N interactions based on such fits in nuclear structure calculations, and can be sizable as illustrated by nuclear matter calculations. Furthermore, we analyzed the Gamow-Teller matrix elements calculated with different chiral forces and  $c_D$  and  $c_E$  values obtained through fits to other observables. We found that it is generally not possible to simultaneously fit all experimental observables even when the uncertainty due to sensitivity to the regulator scheme is taken into account. Our studies indicate that the importance of the regularization scheme and scale in chiral many-body currents needs to be studied more carefully than in previous works, and can lead to additional uncertainties in the many-body calculations. Further studies need to be performed in order to work out a consistent way of regularizing chiral forces and currents.

*Acknowledgments.* We thank R. J. Furnstahl, D. Gazit and K. A. Wendt for useful discussions. This work was supported by the DFG through Grant SFB 1245, the ERC Grant No. 307986 STRONGINT, and the JSPS Grant-in-Aid for Scientific Research No. 26-04323. JM was also supported by an International Research Fellowship from JSPS. AC acknowledges support by the Alexander von Humboldt Foundation through a Humboldt Research Fellowship for Postdoctoral Researchers.

- 
- [1] A. Gezerlis, I. Tews, E. Epelbaum, S. Gandolfi, K. Hebeler, A. Nogga, and A. Schwenk, Phys. Rev. Lett. **111**, 032501 (2013).  
 [2] A. Ekström, G. R. Jansen, K. A. Wendt, G. Hagen, T. Papenbrock, B. D. Carlsson, C. Forssén, M. Hjorth-

- Jensen, P. Navrátil, and W. Nazarewicz, Phys. Rev. C **91**, 051301(R) (2015).  
 [3] E. Epelbaum, H. Krebs, and U.-G. Meißner, Phys. Rev. Lett. **115**, 122301 (2015).  
 [4] B. D. Carlsson, A. Ekström, C. Forssén, D. F. Strömberg,

- G. R. Jansen, O. Lilja, M. Lindby, B. A. Mattsson, and K. A. Wendt, *Phys. Rev. X* **6**, 011019 (2016).
- [5] E. Epelbaum, H.-W. Hammer, and U.-G. Meißner, *Rev. Mod. Phys.* **81**, 1773 (2009).
- [6] R. Machleidt and D. R. Entem, *Phys. Rep.* **503**, 1 (2011).
- [7] H.-W. Hammer, A. Nogga, and A. Schwenk, *Rev. Mod. Phys.* **85**, 197 (2013).
- [8] S. Bacca and S. Pastore, *J. Phys. G* **41**, 123002 (2014).
- [9] S. Weinberg, *Nucl. Phys. B* **363**, 3 (1991).
- [10] D. R. Entem, N. Kaiser, R. Machleidt, and Y. Nosyk, *Phys. Rev. C* **91**, 014002 (2015).
- [11] S. Ishikawa and M. R. Robilotta, *Phys. Rev. C* **76**, 014006 (2007).
- [12] V. Bernard, E. Epelbaum, H. Krebs, and U.-G. Meißner, *Phys. Rev. C* **77**, 064004 (2008).
- [13] V. Bernard, E. Epelbaum, H. Krebs, and U.-G. Meißner, *Phys. Rev. C* **84**, 054001 (2011).
- [14] E. Epelbaum, *Phys. Lett. B* **639**, 456 (2006).
- [15] H. Krebs, E. Epelbaum, and U. G. Meiner, *Annals Phys.* **378**, 317 (2017).
- [16] A. Baroni, L. Girlanda, S. Pastore, R. Schiavilla, and M. Viviani, *Phys. Rev. C* **93**, 015501 (2016).
- [17] S. Kölling, E. Epelbaum, H. Krebs, and U.-G. Meißner, *Phys. Rev. C* **80**, 045502 (2009).
- [18] S. Kölling, E. Epelbaum, H. Krebs, and U.-G. Meißner, *Phys. Rev. C* **84**, 054008 (2011).
- [19] S. Pastore, L. Girlanda, R. Schiavilla, M. Viviani, and R. B. Wiringa, *Phys. Rev. C* **80**, 034004 (2009).
- [20] S. Pastore, L. Girlanda, R. Schiavilla, and M. Viviani, *Phys. Rev. C* **84**, 024001 (2011).
- [21] M. Piarulli, L. Girlanda, L. E. Marcucci, S. Pastore, R. Schiavilla, and M. Viviani, *Phys. Rev. C* **87**, 014006 (2013).
- [22] D. Gazit, S. Quaglioni, and P. Navrátil, *Phys. Rev. Lett.* **103**, 102502 (2009).
- [23] L. E. Marcucci, A. Kievsky, S. Rosati, R. Schiavilla, and M. Viviani, *Phys. Rev. Lett.* **108**, 052502 (2012).
- [24] A. Ekström, G. R. Jansen, K. A. Wendt, G. Hagen, T. Papenbrock, et al., *Phys. Rev. Lett.* **113**, 262504 (2014).
- [25] A. Baroni, L. Girlanda, A. Kievsky, L. E. Marcucci, R. Schiavilla, and M. Viviani, *Phys. Rev. C* **94**, 024003 (2016).
- [26] K. Hebeler, S. K. Bogner, R. J. Furnstahl, A. Nogga, and A. Schwenk, *Phys. Rev. C* **83**, 031301(R) (2011).
- [27] E. Epelbaum, A. Nogga, W. Glöckle, H. Kamada, U.-G. Meißner, and H. Witała, *Phys. Rev. C* **66**, 064001 (2002).
- [28] J. E. Lynn, I. Tews, J. Carlson, S. Gandolfi, A. Gezerlis, K. E. Schmidt, and A. Schwenk, *Phys. Rev. Lett.* **116**, 062501 (2016).
- [29] A. Gardestig and D. R. Phillips, *Phys. Rev. Lett.* **96**, 232301 (2006).
- [30] B. R. Barrett, P. Navrátil, and J. P. Vary, *Prog. Part. Nucl. Phys.* **69**, 131 (2013).
- [31] K. Hebeler, J. D. Holt, J. Menendez, and A. Schwenk, *Ann. Rev. Nucl. Part. Sci.* **65**, 457 (2015).
- [32] P. Navrátil, S. Quaglioni, G. Hupin, C. Romero-Redondo, and A. Calci, *Phys. Scripta* **91**, 053002 (2016).
- [33] H. Hergert, S. K. Bogner, S. Binder, A. Calci, J. Langhammer, et al., *Phys. Rev. C* **87**, 034307 (2013).
- [34] S. Binder, J. Langhammer, A. Calci, and R. Roth, *Phys. Lett. B* **736**, 119 (2014).
- [35] H. Hergert, S. K. Bogner, T. D. Morris, S. Binder, A. Calci, J. Langhammer, and R. Roth, *Phys. Rev. C* **90**, 041302(R) (2014).
- [36] J. Hu, Y. Zhang, E. Epelbaum, U.-G. Meißner, and J. Meng, arXiv:1612.05433.
- [37] G. Hagen et al., *Nature Phys.* **12**, 186 (2016).
- [38] J. Simonis, K. Hebeler, J. D. Holt, J. Menéndez, and A. Schwenk, *Phys. Rev. C* **93**, 011302(R) (2016).
- [39] J. Simonis, S. R. Stroberg, K. Hebeler, J. D. Holt, and A. Schwenk, *Phys. Rev. C* **96**, 014303 (2017).
- [40] C. Drischler, K. Hebeler, and A. Schwenk, *Phys. Rev. C* **93**, 054314 (2016).
- [41] R. F. Garcia Ruiz et al., *Nature Phys.* **12**, 594 (2016).
- [42] G. Hagen, G. R. Jansen, and T. Papenbrock, *Phys. Rev. Lett.* **117**, 172501 (2016).
- [43] J. Birkhan et al., *Phys. Rev. Lett.* **118**, 252501 (2017).
- [44] D. R. Entem and R. Machleidt, *Phys. Rev. C* **68**, 041001(R) (2003).
- [45] P. Navrátil, *Few Body Syst.* **41**, 117 (2007).
- [46] I. Tews, S. Gandolfi, A. Gezerlis, and A. Schwenk, *Phys. Rev. C* **93**, 024305 (2016).
- [47] A. Dyhdalo, R. J. Furnstahl, K. Hebeler, and I. Tews, *Phys. Rev. C* **94**, 034001 (2016).
- [48] L. Coraggio, J. W. Holt, N. Itaco, R. Machleidt, L. E. Marcucci, and F. Sammarruca, *Phys. Rev. C* **89**, 044321 (2014).
- [49] F. Sammarruca, L. Coraggio, J. W. Holt, N. Itaco, R. Machleidt, and L. E. Marcucci, *Phys. Rev. C* **91**, 054311 (2015).
- [50] R. Schiavilla et al., *Phys. Rev. C* **58**, 1263 (1998).
- [51] S. Raman, C. A. Houser, and T. A. Walkiewicz, *At. Data Nucl. Data Tables* **21**, 567 (1978).
- [52] T. S. Park, L. E. Marcucci, R. Schiavilla, M. Viviani, A. Kievsky, S. Rosati, K. Kubodera, D. P. Min, and M. Rho, *Phys. Rev. C* **67**, 055206 (2003).
- [53] S. Ando, T. S. Park, K. Kubodera, and F. Myhrer, *Phys. Lett. B* **533**, 25 (2002).
- [54] M. Hoferichter, P. Klos, and A. Schwenk, *Phys. Lett. B* **746**, 410 (2015).
- [55] D. R. Entem, R. Machleidt, and Y. Nosyk, *Phys. Rev. C* **96**, 024004 (2017).
- [56] A. Nogga, A. Kievsky, H. Kamada, W. Glöckle, L. E. Marcucci, S. Rosati, and M. Viviani, *Phys. Rev. C* **67**, 034004 (2003).
- [57] E. Epelbaum, W. Glöckle, and U.-G. Meißner, *Nucl. Phys. A* **747**, 362 (2005).
- [58] J. Hoppe, C. Drischler, R. J. Furnstahl, K. Hebeler, and A. Schwenk, arXiv:1707.06438.
- [59] E. Epelbaum, *Prog. Part. Nucl. Phys.* **57**, 654 (2006).
- [60] A. Carbone, A. Rios, and A. Polls, *Phys. Rev. C* **90**, 054322 (2014).
- [61] M. Dutra, O. Lourenço, J. S. Sá Martins, A. Delfino, J. R. Stone, and P. D. Stevenson, *Phys. Rev. C* **85**, 035201 (2012).
- [62] E. Epelbaum, H. Krebs, and U.-G. Meißner, *Eur. Phys. J. A* **51**, 53 (2015).
- [63] S. Binder et al., *Phys. Rev. C* **93**, 044002 (2016).
- [64] A. Carbone, A. Cipollone, C. Barbieri, A. Rios, and A. Polls, *Phys. Rev. C* **88**, 054326 (2013).
- [65] M. P. Valderrama and D. R. Phillips, *Phys. Rev. Lett.* **114**, 082502 (2015).

## Erratum: Uncertainties in constraining low-energy constants from ${}^3\text{H}$ $\beta$ decay [Eur. Phys. J. A 53, 168 (2017)]

P. Klos,<sup>1,2,\*</sup> A. Carbone,<sup>1,2,†</sup> K. Hebeler,<sup>1,2,‡</sup> J. Menéndez,<sup>3,§</sup> and A. Schwenk<sup>1,2,4,¶</sup>

<sup>1</sup>*Institut für Kernphysik, Technische Universität Darmstadt, 64289 Darmstadt, Germany*

<sup>2</sup>*ExtreMe Matter Institute EMMI, GSI Helmholtzzentrum für Schwerionenforschung GmbH, 64291 Darmstadt, Germany*

<sup>3</sup>*Department of Physics, University of Tokyo, Hongo, Tokyo 113-0033, Japan*

<sup>4</sup>*Max-Planck-Institut für Kernphysik, Saupfercheckweg 1, 69117 Heidelberg, Germany*

In our article Eur. Phys. J. A 53, 168 (2017) the low-energy constant  $c_D$  in the two-body currents was used incorrectly. The correct definition, which is consistent with the  $c_D$  coupling in the leading three-nucleon forces, gives for Eq. (5):

$$d_R = -\frac{1}{4\Lambda_\chi g_A} c_D + \frac{1}{3}(c_3 + 2c_4) + \frac{1}{6m_N}. \quad (9)$$

As a result the  $c_D$  dependence of the Gamow-Teller matrix elements has changed. Here we provide the corrected Figs. 2–6. While the curves change significantly due to the  $-\frac{1}{4}$  change in the  $c_D$  part of the two-body currents, we emphasize that the discussion provided in our original manuscript remains qualitatively correct, as there is still a strong dependence of the results on the value of  $c_D$ .

We thank R. Schiavilla for pointing out the inconsistent definition of  $c_D$ , and E. Epelbaum and H. Krebs for discussions.

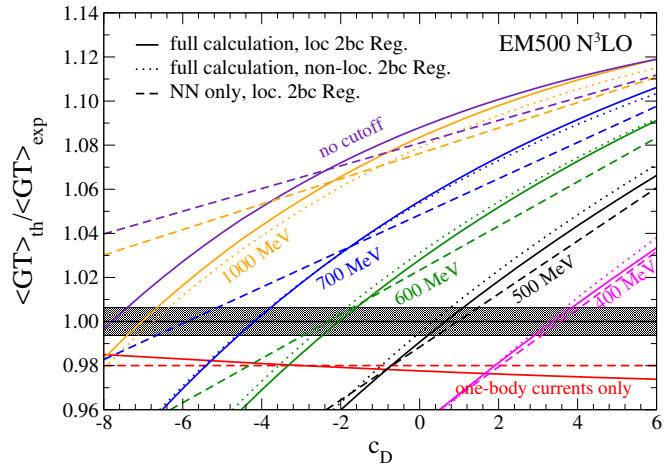


FIG. 2. (Color online) Ratio of calculated and experimental Gamow-Teller matrix elements as a function of  $c_D$  for different cutoff values and regulators in the two-body currents, based on the EM 500 MeV  $\text{N}^3\text{LO}$  potential of Ref. [44]. The solid (dotted) lines show results for nuclear states including 3N forces at  $\text{N}^2\text{LO}$  using the  ${}^3\text{H}$  binding energy constraint of Fig. 1 for a local [non-local with  $n = 2$ , see Eq.(8)] regulator in the two-body currents. For comparison, we also show results based on NN interactions only (dashed lines) and with 1b currents only. The width of the shaded band denotes the  $2\sigma$  experimental uncertainty.

\* pklos@theorie.i kp.physik.tu-darmstadt.de

† arianna@theorie.i kp.physik.tu-darmstadt.de

‡ kai.hebeler@physik.tu-darmstadt.de

§ menendez@nt.phys.s.u-tokyo.ac.jp

¶ schwenk@physik.tu-darmstadt.de



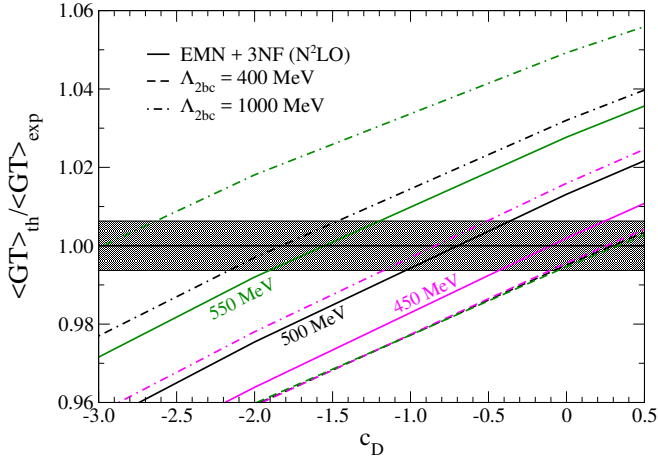


FIG. 3. (Color online) Ratio of calculated and experimental Gamow-Teller matrix elements as a function of  $c_D$  based on the EMN potentials at order  $N^2$ LO of Ref. [55]. We show results for the 2b current cutoff  $\Lambda_{2bc} = 400$  MeV (dashed lines) and  $\Lambda_{2bc} = 1000$  MeV (dash-dotted lines) using a non-local regulator [see Eq.(8)] with  $n = 2$ , whereas the solid lines show the cases when using the same cutoff values in the regulators for the interactions and currents. The width of the shaded band denotes the  $2\sigma$  experimental uncertainty.

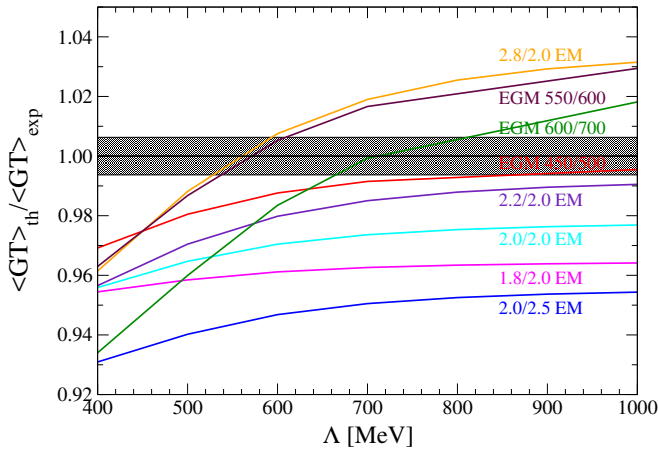


FIG. 4. (Color online) Ratio of calculated and experimental Gamow-Teller matrix elements as a function of the cutoff  $\Lambda$  in the non-local regulator [ $n = 2$ , see Eq. (8)] for a set of chiral interactions, using different fitting observables: the results labeled 'EM' are based on NN plus 3N interactions, for which the  $c_D$  and  $c_E$  values are fit to the binding energy of  ${}^3\text{H}$  and the charge radius of  ${}^4\text{He}$  (see Ref. [26] for details). The results labeled 'EGM' are based on NN plus 3N forces fitted to the binding energy of  ${}^3\text{H}$  and the neutron-deuteron scattering length [59]. The width of the shaded band denotes the  $2\sigma$  experimental uncertainty.

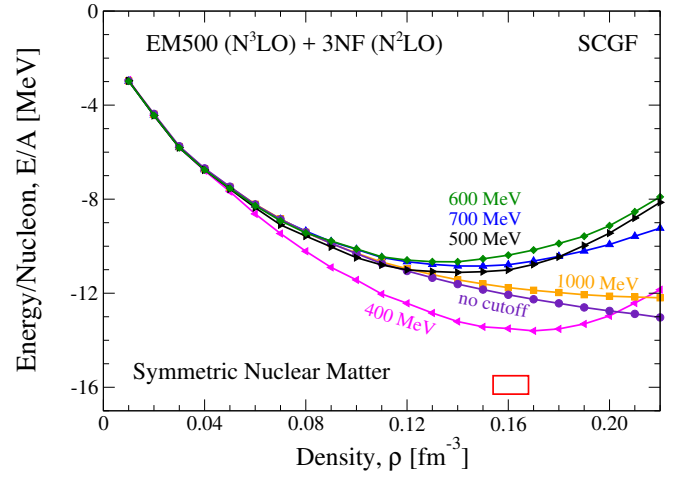


FIG. 5. (Color online) Energy per nucleon of symmetric nuclear matter as a function of nucleon density obtained within the self-consistent Green's function approach [60]. Results are based on the NN EM 500 MeV at  $N^3$ LO, including normal-ordered 3N interaction contributions at  $N^2$ LO. The curves correspond to different  $c_D$  and  $c_E$  values obtained according to Figs. 1 and 2. The box describes the range for the empirical saturation point provided by mean-field calculations [61].

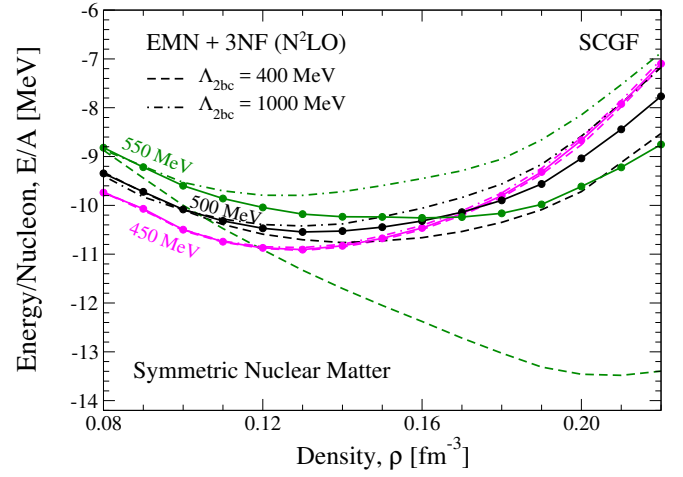


FIG. 6. (Color online) Same as Fig. 5 but showing results based on the EMN potentials at  $N^2$ LO. The curves correspond to different  $c_D$  and  $c_E$  values obtained according to Figs. 1 and 3. The different lines correspond to 2b currents cutoffs equivalent to the interaction (solid),  $\Lambda_{2bc} = 400$  MeV (dashed), and  $\Lambda_{2bc} = 1000$  MeV (dash-dotted) as shown in Fig. 3.